

Developing Carbon Nanofibers from *Gnetum Gnemon Linn* Pericarp Using Dual Activators KOH And Melamine as Innovative Electrode Materials for Supercapacitors

Rakhmawati Farma^{1,*}, Hardini Chania Putri¹, Irma Apriyani¹, Luqyana Adha Azwat², Awitdrus Awitdrus¹, Mohamad Deraman³, Ari Sulisty Rini¹, Rahmondia Nanda Setiadi¹, & Erman Taer¹

¹Department of Physics, University of Riau, Kampus Bina Widya, Km. 12,5 Simpang Baru Pekanbaru, 28293, Riau, Indonesia

²Department of Physics, Universitas Indonesia, Kampus UI Depok, Margonda Raya, Kampus Baru, Depok 16424, Indonesia

³School of Applied Physics, Faculty of Science and Technology, Universiti Kebangsaan Malaysia, 43600 Bangi, Selangor, Malaysia

*Corresponding author: rakhmawati.farma@lecturer.unri.ac.id

Abstract

Synthesis of carbon nanofibers from *Gnetum gnemon Linn* (GP) biomass with dual activators, KOH and melamine, offers a potential approach for high-performance supercapacitor electrodes. This study evaluated the preparation of GP-based carbon nanofibers through single and double activation, with varying melamine masses of 0.1, 0.3, and 0.5 g at 0.3 M KOH. The pyrolysis (integrated carbonization and physical activation) occurred at 600°C in N₂ and 800°C in CO₂ atmospheres. The material was activated using 0.3 g of melamine in 0.3 M KOH to produce abundant and highly amorphous nanofiber structures. These characteristics contributed to the high specific capacitance of 400 F/g at a scan rate of 1 mV/s and an energy density of 17 Wh/kg at a power of 465 W/kg. These results demonstrated the synergistic effect of melamine and KOH in increasing the active surface area and structural conductivity. This finding confirms the potential of GP biomass that has not been optimally utilized as a sustainable precursor for energy storage applications, especially supercapacitors.

Keywords: biomass waste; carbon nanofiber; dual activator; electrode; supercapacitor.

Introduction

In an era where the demand for sustainable energy is growing, we must search for energy storage solutions based on renewable technologies. The depletion of fossil fuels, which are non-renewable and will eventually run out if continued exploitation is undertaken, represents a danger to the security of the world's energy supply (Mei et al., 2024). Although biomass, solar, wind, tidal, and other renewable energy sources present viable answers, each has drawbacks. The wind is unpredictable, the sun only shines for half the day, and the tides only come in at certain times. Biomass has become an intelligent and sustainable carbon source in the face of these difficulties (Rawat et al., 2023). For renewable energy to be used as efficiently as possible, efficient energy storage systems are essential. Recent developments have focused on technologies such as batteries, capacitors, supercapacitors, and fuel cells (Khedulkar et al., 2023). Each technology has unique characteristics; batteries store large amounts of energy, but with low power, capacitors charge quickly but store limited energy, while fuel cells excel in energy storage but lose power density compared to batteries (L. Liu et al., 2022). Of all these options, supercapacitors stand out, combining the advantages of batteries, fuel cells, and capacitors. This makes them a viable option to fulfill future demands for energy storage (B. Wang et al., 2023).

Supercapacitors have high output power, good coulombic efficiency, long cycle stability, and low safety and maintenance, with electrochemical advantages such as fast charging and high specific power. This makes them potential candidates for energy storage in emergency applications in automotive, energy, and communications, although they are still constrained by limited specific energy (S. Wang et al., 2021; Z. Yu et al., 2022). Based on their properties,

supercapacitors can be divided into three primary categories: hybrid capacitors, electrochemical double-layer capacitors (EDLCs), and pseudocapacitors (Lu et al., 2024). In the case of EDLC-type supercapacitor devices, the critical role of electrode materials in determining energy storage performance cannot be overstated. The chosen electrodes must be capable of withstanding rapid charging and discharging cycles with minimal energy loss. Due to its many advantages, activating Carbon is considered the most promising material. Notably, activated Carbon boasts an extensive surface area, facilitating larger charge storage and high conductivity, which ensures efficient charge transfer. Furthermore, its low production cost makes it an economical choice for mass production, coupled with superior thermal resistance, enabling it to remain stable and function effectively at the elevated temperatures often encountered during supercapacitor operation (Fan et al., 2024). Therefore, using activated Carbon as electrode material in EDLC supercapacitors improves the device performance and shows that this technology is a viable and sustainable solution for future energy storage needs.

Furthermore, heteroatom-doped carbon materials have attracted much attention in developing electrodes for energy storage and conversion applications (Huo et al., 2024). Doping heteroatoms such as nitrogen (N), sulfur (S), phosphorus (P), or boron (B) into carbon structures can significantly improve the electrochemical properties of the materials. The presence of heteroatoms can introduce additional active sites, increase surface polarity, and modify the electronic charge distribution, thereby improving electrical conductivity and ion storage capacity (Manasa et al., 2022). In addition, doping can also enhance the wettability of the electrode surface, which is vital to facilitate ion transport during electrochemical processes. Therefore, the heteroatom doping strategy is a practical approach to improving the performance of carbon materials. Interestingly, these doped carbon materials can be obtained through biomass conversion as a raw material for activated Carbon, which is not only environmentally friendly but also has the potential to produce materials with adjustable structure and composition (H. Zhou et al., 2021).

By converting biomass into activated Carbon, many new opportunities exist to utilize previously overlooked natural resources. This innovative process enables the transformation of materials like camellia shells (L. Li et al., 2023), bamboo (Nguyen et al., 2023), turmeric leaves (Chakraborty et al., 2024), Orange peels (H. Liu et al., 2023), *Mangifera indica* seed shells (Farma et al., 2024), and nipa coir (Farma et al., 2023) high-value activated carbon. These materials, often treated as waste, can now serve as valuable precursors in producing activated Carbon, a critical component in various technological applications encompassing energy storage, water purification, and gas separation. As a result, this shift changes how biomass waste is managed, opens the door to new technological industry prospects, drives the circular economy, and supports environmental sustainability through green innovation. The study uses *Gnetum gnemon* Linn pericarp (GP) waste, or melinjo fruit shells, to create activated Carbon for supercapacitor electrodes. *Gnetum gnemon* Linn biomass, a native Indonesian plant, holds significant cultural and practical value within local communities. Melinjo is a prominent commodity with diverse benefits, from culinary use to household materials. While melinjo seeds are commonly utilized, the often-dismissed fruit shells contain valuable compounds like ascorbic acid, polyphenols, and tocopherols, making them excellent candidates for activated carbon production. This presents an innovative solution for biomass waste in Indonesia and underscores the country's capacity to develop sustainable technology using its natural resources.

Biomass-based activated carbon quality is effectively enhanced through dual activators, specifically KOH and melamine. Concurrently employing these activators considerably enhances the material's quality and performance (Che et al., 2023). KOH acts as an activation agent, facilitating the formation and expansion of Carbon's pore structure, resulting in increased specific surface area, adsorption capacity, and improved energy storage performance. Meanwhile, melamine creates active sites on the electrode surface, leading to augmented specific capacitance (C_{sp}) and electrical conductivity. The synergistic effect of these activators not only generates nanostructures like nanofibers, nanoflowers, hierarchical, and nanosheets but also enhances pore structure and storage capacity while improving charge transfer efficiency and electrode stability. This makes it an ideal choice for energy storage applications, particularly supercapacitors, due to its superior performance and enhanced durability.

The development of carbon electrodes using dual activators, KOH and melamine, has significantly improved the supercapacitor's energy storage capabilities. According to a study by (Yang et al., 2020), Activated Carbon made from Chinese fir sawdust by dual activation of KOH and melamine has a power density of 261.44 W/kg and a C_{sp} of 196 F/g, making it an auspicious material for supercapacitors. The utilization of biomass, which was previously regarded as waste, as a valuable source of activated carbon material has become possible thanks to this groundbreaking study. In a later advancement, (Z. Huang et al., 2024) investigated moldy mulberry biomass using a novel dual activator approach that paired melamine with KOH. The results showed a C_{sp} of up to 338 F/g, which was explained by KOH's creation of pore

structure and increased active sites on the carbon surface by melamine. These results were validated and expanded upon in subsequent research by (Q. Li et al., 2021) and (Fang et al., 2019) Utilizing different biomass materials, such as areca nut fiber and lotus stem. The dual activation of KOH and melamine with activated Carbon was used in both investigations, yielding Csp values of 325 F/g and 304 F/g, respectively. Unlike previous studies using biomass such as Chinese fir sawdust, moldy mulberry, areca nut fiber, and lotus stem as carbon sources, this study utilized *Gnetum gnemon* Linn (GP), which is generally rarely reported in the literature. In addition, the dual activation approach using melamine and KOH resulted in a more defined nanofiber structure and higher specific capacitance. For example, compared with biomass-based carbon electrodes reported to have a capacitance of around 196 F/g-338 F/g, the GP-based electrode in this study reached 400 F/g at 1 mV/s. The presence of nanofibers formed by KOH-melamine activation also provides advantages in terms of surface area and more efficient ion diffusion pathways, which have not been widely explored in other biomass studies.

These consistent findings demonstrate the remarkable performance enhancement achieved by combining KOH and melamine activation, confirming the superiority of this method in producing high-performance activated Carbon. In summary, previous studies have conclusively shown that dual activation of KOH and melamine significantly improves activated carbon quality and supercapacitors' performance. However, challenges remain in optimizing this process to achieve maximum storage capacity and exploring this technology's potential applications and development in broader energy storage systems. This project aims to produce carbon nanofibers using GP biomass as a new supercapacitor electrode material. Using the dual activators KOH and melamine, we will adjust the melamine mass to enhance the electrochemical properties, such as specific capacitance. The carbon nanofiber will undergo extensive testing and analysis to assess its performance in supercapacitor applications and advance the creation of more effective and sustainable energy storage.

Experiment

The Manufacturing process for GP

Carbon material involves several crucial steps to ensure optimal water removal and material stability, as shown in Figure 1. Beginning with sun drying, the biomass undergoes preheating at 200°C for three hours to initiate the formation of the basic carbon structure and eliminate volatile compounds. Subsequently, the material goes through a ball milling process to grind the Carbon into a micron-sized powder for even distribution of the activator material during chemical activation.

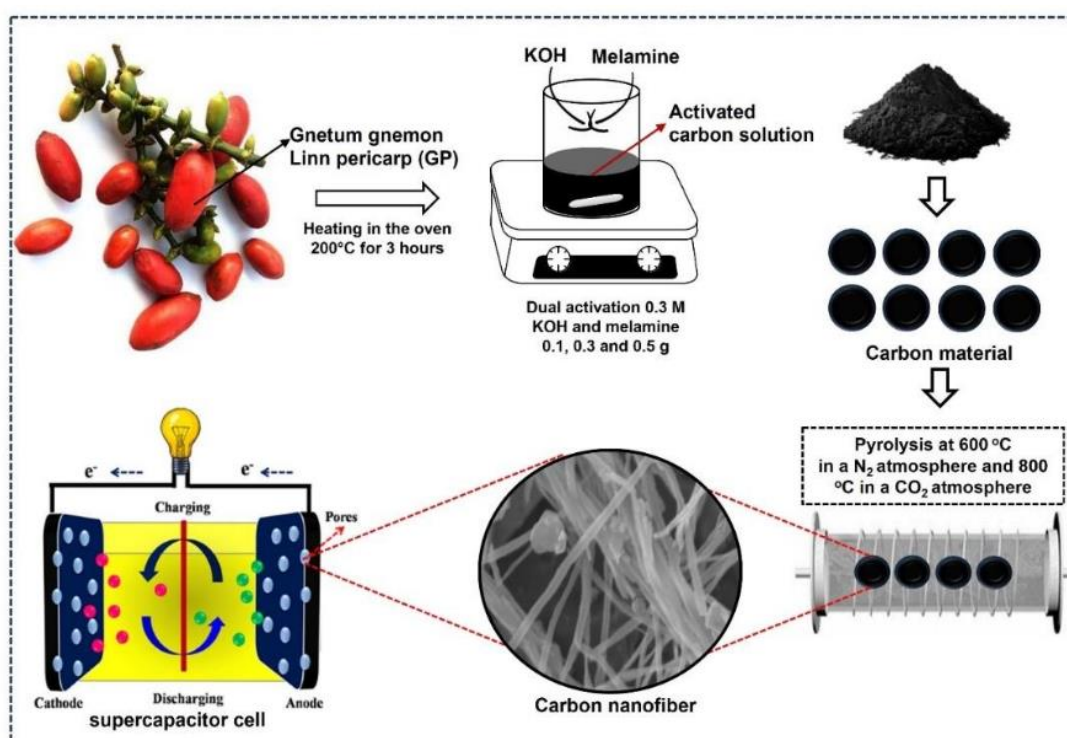


Figure 1 Schematic of the manufacture of GP carbon material with dual activation of KOH and melamine for supercapacitors.

The fine carbon powder is then activated using a combination of dual activators, 0.3 M KOH, and melamine, with masses of 0.1, 0.3, and 0.5 g, to maximize pore development and surface characteristics essential for electrochemical performance. After activation, the carbon powder is compressed into a coin shape to ensure material density and homogeneity during pyrolysis. Primary pyrolysis occurs in a nitrogen atmosphere at 600°C to increase carbon purity and structural integrity. The secondary pyrolysis stage is carried out using carbon dioxide gas at 800°C to expand the pores further, create new pores, and increase the specific surface area of the material. These steps are designed to produce GP carbon material optimized for supercapacitor applications.

Characterization of carbon materials

Scanning electron microscopy with a JEOL JSM-6510 LA instrument was used for topographic analysis. Magnifications of 5000x and 40000x were used to analyze the surface morphology thoroughly. The elemental composition of the GP was ascertained using energy-dispersive X-ray analysis with the same apparatus in the 0–6 keV energy range. Using a Shimadzu Prestige-21 IR, Fourier Transform Infrared spectroscopy revealed functional groups in the GP samples over the 500–4500 cm^{-1} wavenumber range, providing information about their chemical bonding. Using a Shimadzu 700 XRD apparatus, the crystallographic phase structure was analyzed using X-ray diffraction (XRD) scans at 2θ angles ranging from 10° to 60° to evaluate the material's crystallinity. N_2 adsorption-desorption measurements were also conducted to evaluate the specific surface area and pore size distribution using a Quantachrome TouchWin v1.22 on a NOVA touch 4LX system. The samples were outgassed at 300°C for three hours, providing essential data on their porosity characteristics.

Electrochemical measurements

The two electrodes in the symmetric two-electrode supercapacitor cell comprised the same GP carbon material. A chicken eggshell membrane was positioned between them to promote ion transport during the charge-discharge process while avoiding direct contact between the electrodes. A 1 M H_2SO_4 electrolyte was employed. Bilayer capacitance was collected using a 316 L stainless steel current collector. Galvanostatic Charge-Discharge (GCD) and Cyclic Voltammetry (CV) methods were used to characterize the device. While GCD testing was conducted at a current density of 1–10 A/g within the same voltage range, CV measurements were performed at a scan rate of 1–100 mV/s within a potential range of 0–1 V. These evaluations aimed to assess the capacitance response, electrode performance, and specific capacitance under various operating conditions.

Result

SEM analysis was performed to observe the surface morphology of GP carbon electrodes synthesized using single and dual activators at magnifications of 5000x and 40,000x, as shown in Figure 2. Figures 2 (a) and (d) show the surface morphology of GP carbon electrodes with a nanofiber structure formed due to KOH activation in the carbon matrix. However, the number of nanofibers formed was relatively small, possibly due to the use of KOH as a single activator without the addition of melamine. Figures 2 (b) and (e) show a clearer morphological difference in the GP-03 carbon electrode, which displays a greater number of nanofibers compared to GP and GP-05. Meanwhile, Figures 2 (c) and (f) show the morphology of GP-05 with fewer nanofibers than GP-03. Figure 3 shows the chemical content and EDX spectrum of the GP material. This spectrum indicates the presence of Carbon (C), oxygen (O), and potassium (K).

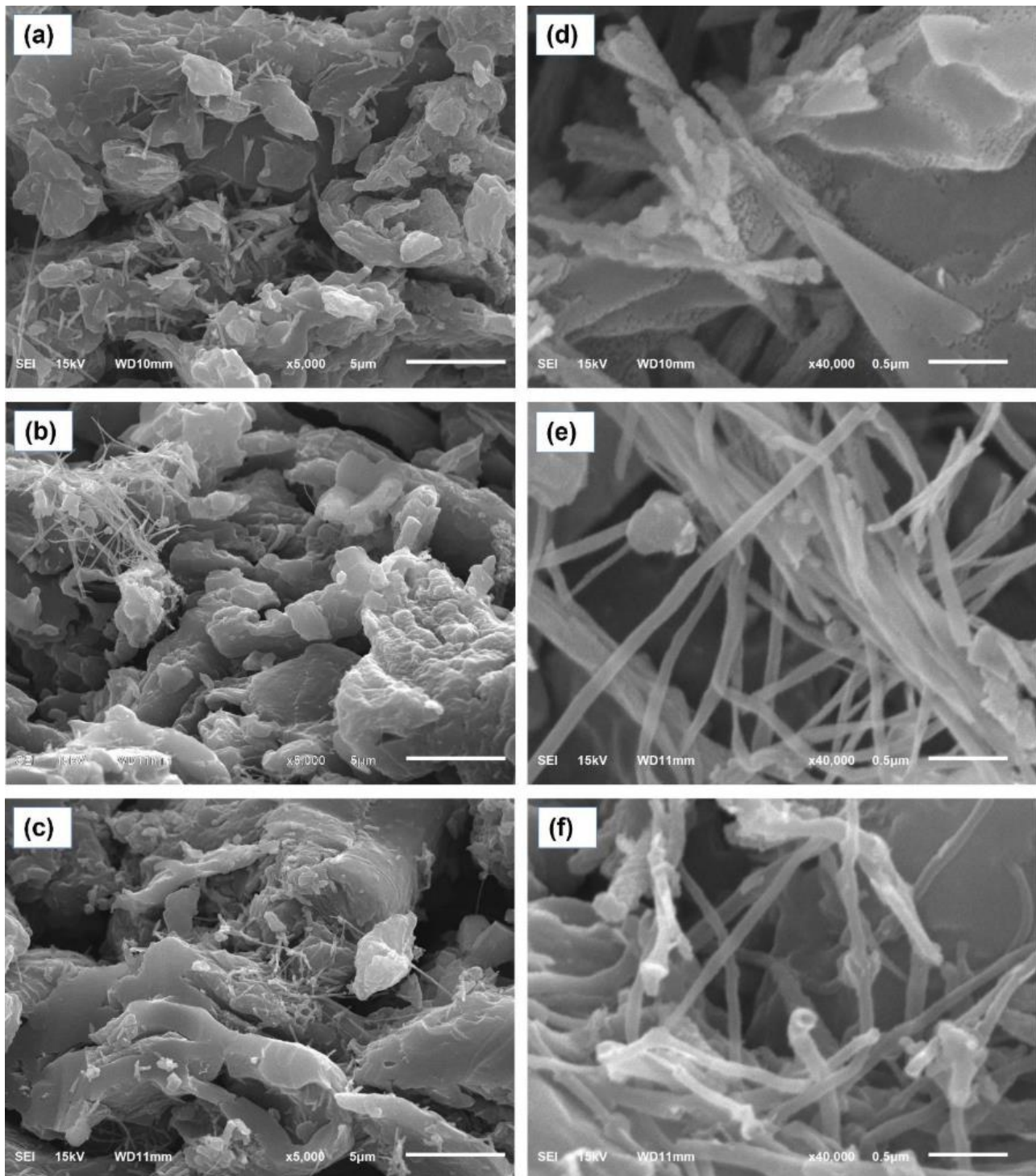


Figure 2 Surface morphology at 5000x magnification (a) GP (b) GP-03 (c) GP-05 and 40000x magnification (d) GP (e) GP-03 (f) GP-05.

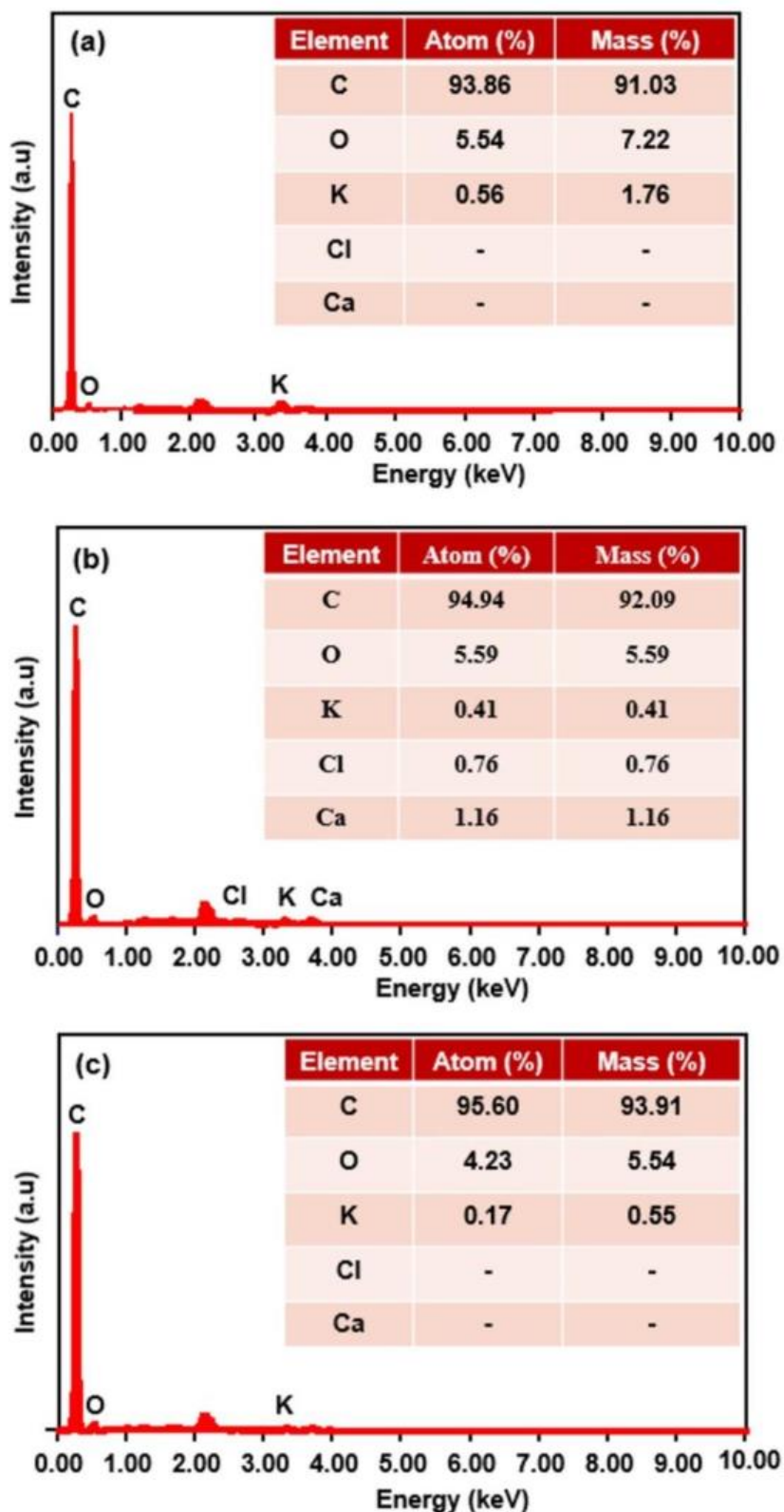


Figure 3 EDX spectrum (a) GP (b) GP-03 (c) GP-05.

Figure 4 presents the FTIR and XRD spectra, as well as the N_2 adsorption–desorption isotherms and pore size distribution. The functional groups of GP can be seen in the FTIR spectra in the wavenumber region of $450\text{--}4500\text{ cm}^{-1}$ (Figure 4 (a)), consisting of O-H, $C\equiv C$, and $C=C$. The microstructure of the GP carbon electrodes was visible through XRD examination, as shown in Figure 4(b). Significant peaks produced by all samples at 2θ angles of 22 and 44° ,

corresponding to the (002) and (100) scattering planes, respectively, confirm the presence of an amorphous structure (Cao et al., 2021). The BET method was also used at 77K to analyze the GP electrodes' pore structure and surface area. The isothermal curve in Figure 4(c) illustrates the results, revealing a considerable surface area and pore architecture shift. According to the IUPAC classification, the curve shows traits of both type I and type IV isotherms, indicating the coexistence of microporous and mesoporous structures within the carbon matrix (Nayak et al., 2024). The BET method was utilized to determine the total specific surface area of the carbon electrodes, GP-03, GP-05, and 34.395 m²/g, 445.591 m²/g, and 470.96 m²/g. The corresponding pore volumes were 0.015 cc/g, 0.024 cc/g, and 0.018 cc/g. These findings show that GP-03 has the most enormous pore volume, and GP-05 has the largest surface area. Furthermore, it is crucial to remember that capacitance saturation, which lowers C_{sp}, can occur in supercapacitor cells, meaning that high surface area is not necessarily directly correlated with capacitive characteristics. Saturation occurs due to damaged pore walls and huge pore diameters. The pore sizes of the samples are distributed, with average diameters of 4.4 nm, 4.08 nm, and 3.2 nm, as shown in Figure 4 (d). This indicates that mesopores are most abundantly distributed on the surface of the carbon matrix. This ensures that the absorption and transport of ions are running well (Shanmuga Priya et al., 2020).

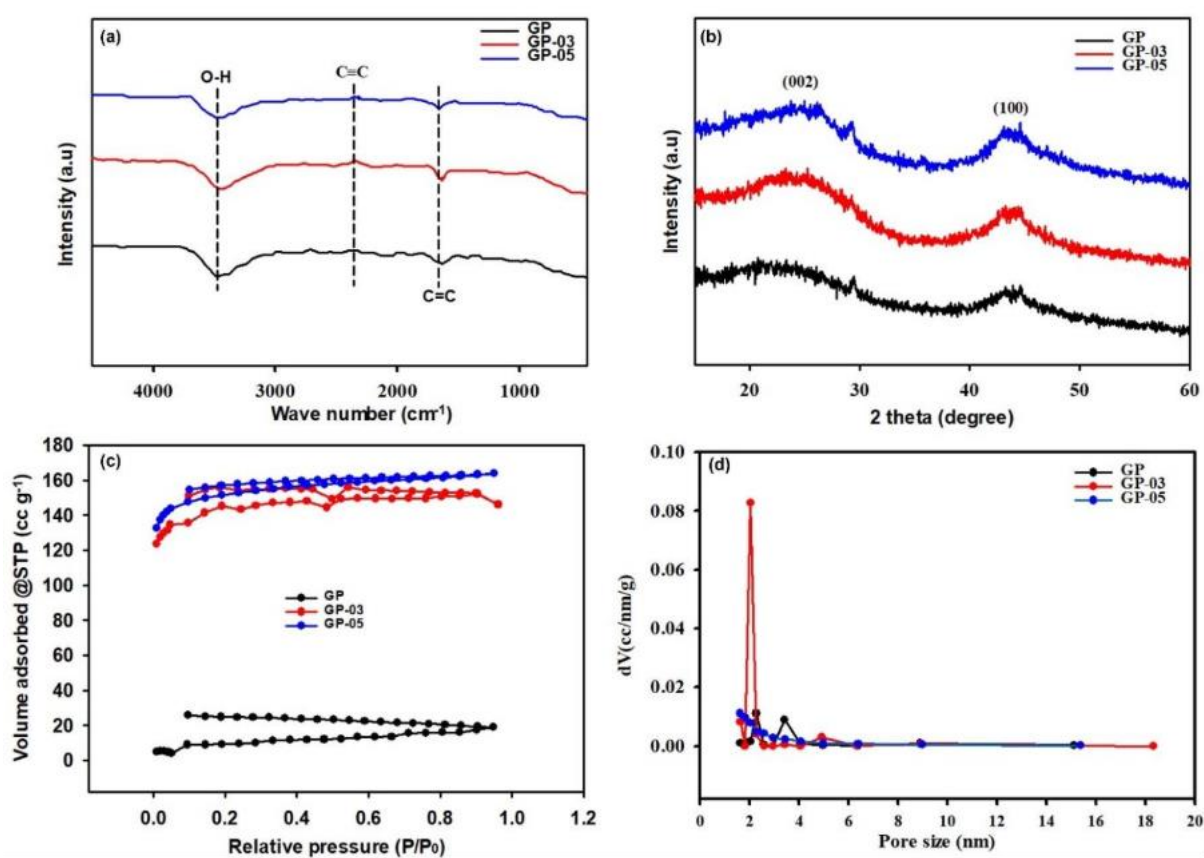


Figure 4 (a) FTIR spectrum, (b) XRD spectrum, (c) N₂ adsorption-desorption, (d) pore size distribution.

Determining the C_{sp} and examining the carbon electrode performance level in GP biomass-based supercapacitor cells with single and dual activators in a 1M H₂SO₄ atmosphere depend heavily on the CV measurement. An electric double-layer capacitor's optimal shape is a quasi-rectangular CV curve, which is the outcome (S. Huang et al., 2023). Figure 5 (b) shows the CV curve of GP-03 at various scan rates. At this scan rate, the curve remains rectangular and shows perfect capacitance behavior, a general characteristic of double-layer electrical capacitors (Q. X. Yu et al., 2023). GP-03's constant curve forms indicate stability under various operating settings, which validates its potential for supercapacitor applications. Additionally, Figure 5 (c) shows the link between each sample's scan rate and CSP value. Higher CSPs are attained at low scan rates because there is enough time for electrolyte ion diffusion into the electrode's accessible pores. On the other hand, ion accessibility falls with increasing scan rate, which lowers the C_{sp} (Khalid et al., 2020). At a scan rate of 100 mV/s, GP-03 has a C_{sp} of only 20 F/g.

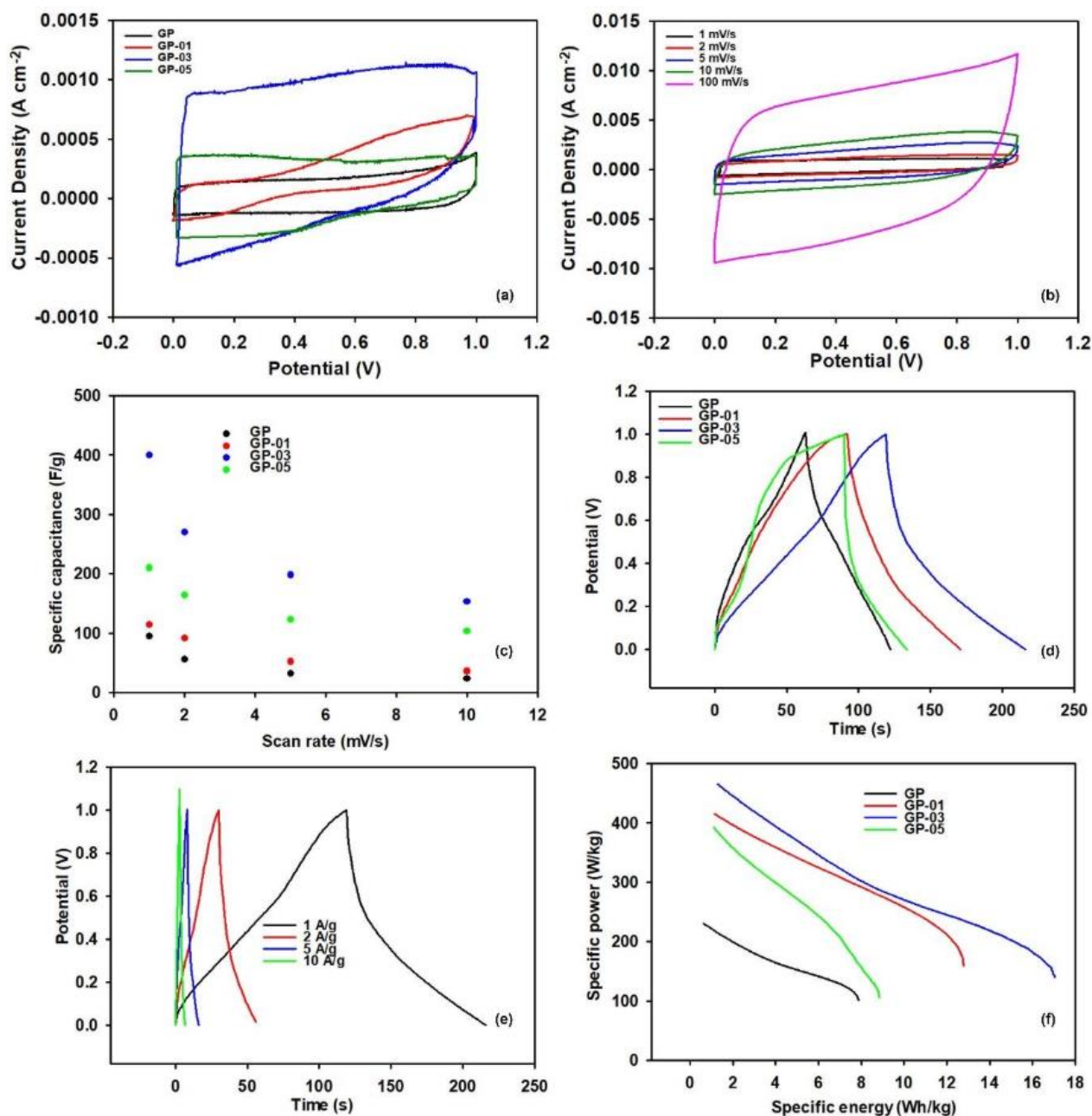


Figure 5 CV curves (a) GP, (b) GP-03, (c) graph of scan rate versus C_{sp} , GCD curves (d) GP, (e) GP-03, (f) Ragone plot.

GCD measurements provide a thorough assessment for further analysis to assess the capacitive characteristics of carbon electrodes in GP-based supercapacitor cells, as seen in Figure 5(d). The measurement results show an asymmetric triangular shape with linear traits, indicating the presence of electric double-layer electrochemical capacitor (EDLC) properties (Raj et al., 2020). The small voltage drop is attributed to the abundant nanofiber structure and high pore volume, contributing to the low equivalent series resistance (Inayat et al., 2023). The GCD curves of the carbon electrode at various current densities are shown in Figure 5(e). Electric double-layer capacitance supercapacitors are characterized by linear, asymmetric triangle forms in their curves. The curves exhibit shape retention from 1 to 10 A/g as the current density increases, suggesting that the carbon electrode maintains its capacitive characteristics under different loads (Du et al., 2024). The stability of the electrode, which is necessary for high-efficiency energy storage applications in supercapacitors, is reflected in this consistency. For the GP sample, a power density of 465 W/kg and a power density of 17 Wh/kg are shown in the Ragone diagram, as shown in Figure 5 (f).

Discussion

During the activation process, KOH reacts to form K_2CO_3 , which is further reduced by Carbon, producing K, K_2O , CO, and CO_2 , and generating additional pores in the structure (Jia et al., 2022). This series of reactions contributes to the matrix's degradation and aggregation of ascorbic acid, yielding micro-sized fibers. Removing tightly bound hydrogen can further refine these microfibers into nanofibers (J. Wang et al., 2020). Adding melamine ($C_3N_6H_6$) is instrumental in engendering nanofiber structures in the carbon matrix. This compound can undergo condensation to form graphite nitride ($g-C_3N_4$) and re-agglomerate ascorbic acid, resulting in a nanofiber-rich structure. Incorporating nanofiber structures into carbon electrodes offers excellent potential to enhance supercapacitors' electrochemical performance. These structures provide outstanding electrical properties, flexibility, conductivity, and chemical stability. They facilitate efficient ion transport and improve electron mobility through interconnected networks. Additionally, the presence of nanofibers expands the available surface area for active sites, reduces the distance for ion movement, and lowers ion diffusion resistance. As a buffer to hold electrolyte ions, the nanofiber architecture contributes significantly to faster capacitive response and improved kinetics in supercapacitor cells (C. Huang et al., 2023). However, using melamine with a mass ratio exceeding 0.3 g can block the pore channels and ultimately inhibit the formation of nanofibers.

The carbon content comes from the basic GP biomass, rich in organic compounds such as ascorbic acid, polyphenols, and tocopherols, which are carbonized through pyrolysis. Carbon is the dominant element in single- and double-activator carbon electrodes, which provide good electrical conductivity and show the great potential of GP biomass as a carbon source for electrodes. The oxygen element comes from the degradation of compounds, ascorbic acid ($C_6H_8O_6$), polyphenols ($C_{21}H_{20}O_6$), and tocopherols ($C_{29}H_{50}O_2$), which are the basic contents of GP biomass during the chemical activation and pyrolysis processes (Ma et al., 2019). Oxygen also increases the wettability between the electrode and electrolyte during the supercapacitor cells' charging and discharging process, as explained by (Gopalakrishnan & Badhulika, 2020). The potassium element comes from using a KOH activator during the chemical activation process, as reported by (X. Zhou et al., 2020). Interestingly, the GP-03 carbon electrode also contains a small amount of calcium (Ca) and chlorine (Cl) minerals in the carbon lattice framework, which originates from the elemental composition of biomass, as found by (Farma et al., 2021). The presence of Ca can make a positive contribution to the structure and performance of the electrode because the calcium carbonate compound ($CaCO_3$) naturally contained in the shell can be decomposed during the carbonization process and function as a templating agent for pore formation, which is very beneficial for increasing the active surface area and facilitating the diffusion of electrolyte ions in supercapacitor applications (Armynah et al., 2024). On the other hand, the detected Cl element is likely to come from the residual chemical activator and does not make a significant electrochemical contribution.

The O-H functional group is characterized by absorption at wavenumber $3620.54-2565.44\text{ cm}^{-1}$, which is caused by stretching vibrations. This indicates the breakdown of adsorbed hydroxyl and water, generating strong hydrogen bonds in the sample and aromatic compounds as carbon components (Han et al., 2021). Additionally, the absorption at 2376.40 cm^{-1} indicates the existence of $C\equiv C$ functional groups, indicating high carbon purity due to the pyrolysis process's loss of hydrogen and oxygen, which raises the material's conductivity (Mehdi et al., 2023). Furthermore, the absorption at 1595.20 cm^{-1} shows that the pyrolysis process releases O or H elements, indicating high carbon purity. This stretching of the $C=C$ functional group is typical of aromatic ring compounds in activated carbon-based electrodes (Chen et al., 2021). O-H wettability improves supercapacitor performance because it helps electrolyte ions to be absorbed and transported into the carbon pores. In addition, these functional groups are significant in enhancing supercapacitors' electrochemical performance because the aromatization reaction increases the carbon pores (Okonkwo et al., 2020).

A steep increase in adsorption at relative pressures below 0.1 indicates the presence of micropores, while the gradual rise in adsorption between 0.1 and 0.9 confirms the contribution of mesopores (Fu et al., 2021). The GP-03 and GP-05 carbon electrodes exhibit significantly more noticeable hysteresis than GP, indicating a greater presence of micro-mesopores on their surfaces. Micropores help achieve high specific surface areas and increase charge deficiency locations because they function as reservoirs, shorten ion transport pathways, and accelerate ion transport rates (F. Liu et al., 2019). The unperfected or unclosed loop shape on the curve indicates the presence of trapped N_2 gas in the smaller pores. The nitrogen affinity in the GP sample, caused by its heterogeneous surface nature, hinders the release of the trapped N_2 gas. This is related to the pore structure, which resembles a narrow-necked bottle with a wide body shape (Yuan et al., 2022).

The area of the CV curve represents the C_{sp} ; GP-03 has the largest area and the highest C_{sp} value of 400 F/g. Many nanofibers may be produced using 0.3 M KOH and 0.3 g melamine dual activators, improving the electrochemical process's efficiency and providing the best possible structure for storing charge. Nevertheless, melamine concentrations of more than 0.3 g cause erosion of the nanofiber wall, which reduces the number of nanofibers and lowers capacitance

and charge storage capacity (Ramesh et al., 2021). The decrease in specific capacitance from 400 F/g at 1 mV/s to 20 F/g at 100 mV/s indicates that the electrode material experiences a reduced charge storage efficiency at high scan rates. This phenomenon is common in carbon-based materials, especially when the ion transport process into the active pores is limited to a very short cycle time. This indicates that most of the charges are stored through surface adsorption. These findings highlight the importance of maximizing the scan rate to get the most out of the carbon matrix for energy storage applications. The GP-03 carbon electrode showed longer charge and discharge times than other samples, indicating better storage capacity. This also aligns with the CV measurements that showed consistent electrochemical behavior. This phenomenon is due to the abundance of nanofibers in the material structure. These nanofibers increase the C_{sp} because they provide a larger surface area for charge storage, allow more efficient ion diffusion, and support optimal electrostatic charge storage without involving redox reactions (Wei et al., 2024).

Conclusion

The study definitively identifies electrode materials for energy storage technology using biomass waste. It effectively produces carbon nanofibers from GP biomass through a dual activation process. These groundbreaking electrode materials demonstrate superior performance for supercapacitor applications. The single activation process uses 0.3 M KOH, while the dual activation process employs a combination of 0.3 M KOH and melamine with varying masses of 0.1, 0.3, and 0.5 g. Combining KOH and melamine activators conclusively proves effective in creating nanofiber structures through high-temperature pyrolysis. According to this research, melinjo fruit shell biomass waste can be used as an electrode material in the dual activation method of contemporary energy storage technology to improve energy efficiency. The study shows that the resulting electrode material has a power density of 465 W/kg and a high C_{sp} of 400 F/g.

Acknowledgments

The authors would like to thank DRPM Kemenristek/BRIN, Republic of Indonesia, for the financial support through the first-year project of the Fundamental research contract number 102/C3/DT.05.00/PL/2025, derivative contract 19575/UN19.5.1.3/AL.04/2025, Furthermore, the authors thank the National Research and Innovation Agency (BRIN) for financial support through the collaboration center project, contract number 04/PPK.KP/PKR.GEL.VII/II/2025.

Compliance with ethics guidelines

The authors declare they have no conflict of interest or financial conflicts to disclose.

This article contains no studies with human or animal subjects performed by the authors.

References

- Armynah, B., Nairanti, D., Agustino, A., Taer, E., & Tahir, D. (2024). Discarded Persea americana leaf-derived natural O, Mg, and Ca self-doped activated carbon and its applications as electrode materials for high-performance symmetric supercapacitors. *Diamond and Related Materials*, 143, 110879. <https://doi.org/10.1016/j.diamond.2024.110879>
- Cao, L., Li, H., Xu, Z., Zhang, H., Ding, L., Wang, S., Zhang, G., Hou, H., Xu, W., Yang, F., & Jiang, S. (2021). Comparison of the heteroatoms-doped biomass-derived carbon prepared by one-step nitrogen-containing activator for high performance supercapacitor. *Diamond and Related Materials*, 114, 108316. <https://doi.org/10.1016/j.diamond.2021.108316>
- Chakraborty, R., Sharma, A., Maji, P. K., Rudra, S., Kumar Nayak, A., Nath Chatterjee, P., Naik Banothu, Y., & Pradhan, M. (2024). Nitrogen and oxygen self-doped hierarchical porous carbon nanosheets derived from turmeric leaves for high-performance supercapacitor. *Inorganica Chimica Acta*, 567, 122056. <https://doi.org/10.1016/j.ica.2024.122056>
- Che, C., Lv, Y., Wu, X., Dong, P., Liang, N., Gao, H., & Guo, J. (2023). A dual-template strategy assisted synthesis of porous coal-based carbon nanofibers for supercapacitors. *Diamond and Related Materials*, 137, 110140. <https://doi.org/10.1016/j.diamond.2023.110140>

- Chen, T., Luo, L., Luo, L., Deng, J., Wu, X., Fan, M., Du, G., & Zhao, W. (2021). High energy density supercapacitors with hierarchical nitrogen-doped porous carbon as active material obtained from bio-waste. *Renewable Energy*, 175, 760-769. <https://doi.org/10.1016/j.renene.2021.05.006>
- Du, H., Yang, Y., Zhang, C., Li, Y., Wang, J., Zhao, K., Lu, C., Sun, D., Lu, C., Chen, S., & Ma, X. (2024). Hierarchical porous carbon originated from the directing associated with activation as high-performance electrodes for supercapacitor and Li ion capacitor. *Journal of Power Sources*, 614, 234988. <https://doi.org/10.1016/j.jpowsour.2024.234988>
- Fan, Y., Fu, F., Yang, D., Liu, W., & Qiu, X. (2024). Thiocyanogen-modulated N, S Co-doped lignin hierarchical porous carbons for high-performance aqueous supercapacitors. *Journal of Colloid and Interface Science*, 667, 147-156. <https://doi.org/10.1016/j.jcis.2024.04.099>
- Fang, J., Guo, D., Kang, C., Wan, S., Li, S., Fu, L., Liu, G., & Liu, Q. (2019). Enhanced hetero-elements doping content in biomass waste-derived carbon for high performance supercapacitor. *International Journal of Energy Research*, 43(14), 8811-8821. <https://doi.org/10.1002/er.4834>
- Farma, R., Apriyani, I., Deraman, M., Taer, E., Nanda, R., & Sulisty, A. (2023). Enhanced electrochemical performance of oxygen, nitrogen, and sulfur doped Nypa fruticans-based carbon nanofiber for high performance supercapacitors. *Journal of Energy Storage*, 67, 107611. <https://doi.org/10.1016/j.est.2023.107611>
- Farma, R., Maurani, S. F., Apriyani, I., Awitdrus, Yanuar, & Rini, A. S. (2021). Fabrication of carbon electrodes from sago midrib biomass with chemical variation for supercapacitor cell application. *Journal of Physics: Conference Series*, 2049(1), 1-10 <https://doi.org/10.1088/1742-6596/2049/1/012054>
- Farma, R., Refieyana, C., & Apriyani, I. (2024). Biomass valorization of Mangifera Indica into hierarchical carbon materials with self-doping oxygen assisted carbonization for supercapacitor applications. *Energy Sources, Part A: Recovery, Utilization and Environmental Effects*, 46(1), 5168-5179. <https://doi.org/10.1080/15567036.2024.2336176>
- Fu, S., Fang, Q., Li, A., Li, Z., Han, J., Dang, X., & Han, W. (2021). Accurate characterization of full pore size distribution of tight sandstones by low-temperature nitrogen gas adsorption and high-pressure mercury intrusion combination method. *Energy Science and Engineering*, 9(1), 80-100. <https://doi.org/10.1002/ese3.817>
- Gopalakrishnan, A., & Badhulika, S. (2020). Effect of self-doped heteroatoms on the performance of biomass-derived carbon for supercapacitor applications. *Journal of Power Sources*, 480, 228830. <https://doi.org/10.1016/j.jpowsour.2020.228830>
- Han, Q., Wang, X., Gao, N., Wang, X., Chen, C., Xu, B., & Ma, F. (2021). Quantitative determination of ractopamine in swine urine using Fourier transform infrared (FT-IR) spectroscopy analysis. *Infrared Physics and Technology*, 113, 103653. <https://doi.org/10.1016/j.infrared.2021.103653>
- Huang, C., Su, Y., Gong, H., Jiang, Y., Chen, B., Xie, Z., Zhou, J., & Li, Y. (2023). Biomass-derived multifunctional nanoscale carbon fibers toward fire warning sensors, supercapacitors and moist-electric generators. *International Journal of Biological Macromolecules*, 256 (1). <https://doi.org/10.1016/j.ijbiomac.2023.127878>
- Huang, S., Qiu, X. Q., Wang, C. W., Zhong, L., Zhang, Z. H., Yang, S. S., Sun, S. R., Yang, D. J., & Zhang, W. L. (2023). Biomass-derived carbon anodes for sodium-ion batteries. *Xinxing Tan Cailiao/New Carbon Materials*, 38(1), 40-72. [https://doi.org/10.1016/S1872-5805\(23\)60718-8](https://doi.org/10.1016/S1872-5805(23)60718-8)
- Huang, Z., Chen, J., Chen, H., Wan, H., Yang, Y., Fan, T., Zhang, Q., Jin, H., Wang, J., & Wang, S. (2024). Tailoring moldy-mulberry-derived carbons for ionic liquid-based supercapacitors with ultrahigh energy density. *Diamond and Related Materials*, 144. <https://doi.org/10.1016/j.diamond.2024.110994>
- Huo, L., Lv, M., Li, M., Ni, X., Guan, J., Liu, J., Mei, S., Yang, Y., Zhu, M., Feng, Q., Geng, P., Hou, J., Huang, N., Liu, W., Kong, X. Y., Zheng, Y., & Ye, L. (2024). Amorphous MnO₂ Lamellae Encapsulated Covalent Triazine Polymer-Derived Multi-Heteroatoms-Doped Carbon for ORR/OER Bifunctional Electrocatalysis. *Advanced Materials*, 36(18). <https://doi.org/10.1002/adma.202312868>
- Inayat, A., Albalawi, K., Rehman, A. ur, Adnan, Saad, A. Y., Saleh, E. A. M., Alamri, M. A., El-Zahhar, A. A., Haider, A., & Abbas, S. M. (2023). Tunable synthesis of carbon quantum dots from the biomass of spent tea leaves as supercapacitor electrode. *Materials Today Communications*, 34, 105479. <https://doi.org/10.1016/j.mtcomm.2023.105479>
- Jia, B., Mian, Q., Wu, D., & Wang, T. (2022). Heteroatoms self-doped porous carbon from cottonseed meal using K₂CO₃ as activator and DES electrolyte for supercapacitor with high energy density. *Materials Today Chemistry*, 24, 100828. <https://doi.org/10.1016/j.mtchem.2022.100828>
- Khalid, M., Paul, R., Honorato, A. M. B., & Varela, H. (2020). Pinus nigra pine derived hierarchical carbon foam for high performance supercapacitors. *Journal of Electroanalytical Chemistry*, 863, 114053. <https://doi.org/10.1016/j.jelechem.2020.114053>

- Khedulkar, A. P., Pandit, B., Dang, V. D., & Doong, R. . (2023). Agricultural waste to real worth biochar as a sustainable material for supercapacitor. *Science of the Total Environment*, 869, 161441. <https://doi.org/10.1016/j.scitotenv.2023.161441>
- Li, L., Zheng, X., Zhang, F., Yu, H., Wang, H., Jia, Z., Sun, Y., Jiang, E., & Xu, X. (2023). Formamide hydrothermal pretreatment assisted camellia shell for upgrading to N-containing chemical and supercapacitor electrode preparation using the residue. *Energy*, 265, 126247. <https://doi.org/10.1016/j.energy.2022.126247>
- Li, Q., Lu, T., Wang, L., Pang, R., Shao, J., Liu, L., & Hu, X. (2021). Biomass based N-doped porous carbons as efficient CO₂ adsorbents and high-performance supercapacitor electrodes. *Separation and Purification Technology*, 275, 119204. <https://doi.org/10.1016/j.seppur.2021.119204>
- Liu, F., Gao, Y., Zhang, C., Huang, H., Yan, C., Chu, X., Xu, Z., Wang, Z., Zhang, H., Xiao, X., & Yang, W. (2019). Highly microporous carbon with nitrogen-doping derived from natural biowaste for high-performance flexible solid-state supercapacitor. *Journal of Colloid and Interface Science*, 548, 322–332. <https://doi.org/10.1016/j.jcis.2019.04.005>
- Liu, H., Huang, X., Zhou, M., Gu, J., Xu, M., Jiang, L., Zheng, M., Li, S., & Miao, Z. (2023). Efficient conversion of biomass waste to N/O co-doped hierarchical porous carbon for high performance supercapacitors. *Journal of Analytical and Applied Pyrolysis*, 169, 105844. <https://doi.org/10.1016/j.jaap.2022.105844>
- Liu, L., An, X., Tian, Z., Yang, G., Nie, S., Shang, Z., Cao, H., Cheng, Z., Wang, S., Liu, H., & Ni, Y. (2022). Biomass derived carbonaceous materials with tailored superstructures designed for advanced supercapacitor electrodes. *Industrial Crops and Products*, 187(PB), 115457. <https://doi.org/10.1016/j.indcrop.2022.115457>
- Lu, S., Xiao, Q., Yang, W., Wang, X., Guo, T., Xie, Q., & Ruan, Y. (2024). Multi-heteroatom-doped porous carbon with high surface adsorption energy of potassium derived from biomass waste for high-performance supercapacitors. *International Journal of Biological Macromolecules*, 258, 128794. <https://doi.org/10.1016/j.ijbiomac.2023.128794>
- Ma, Z., Yang, Y., Wu, Y., Xu, J., Peng, H., Liu, X., Zhang, W., & Wang, S. (2019). In-depth comparison of the physicochemical characteristics of bio-char derived from biomass pseudo components: Hemicellulose, cellulose, and lignin. *Journal of Analytical and Applied Pyrolysis*, 140, 195–204. <https://doi.org/10.1016/j.jaap.2019.03.015>
- Manasa, P., Sambasivam, S., & Ran, F. (2022). Recent progress on biomass waste derived activated carbon electrode materials for supercapacitors applications — A review. *Journal of Energy Storage*, 54, 105290. <https://doi.org/10.1016/j.est.2022.105290>
- Mehdi, R., Raza, S., Hussain, A., & Hussain, R. (2023). Biomass derived activated carbon by chemical surface modification as a source of clean energy for supercapacitor application. *Fuel*, 348, 128529. <https://doi.org/10.1016/j.fuel.2023.128529>
- Mei, Y., Liu, S., Wu, L., Zhou, B., Wang, Z., Huang, Z. H., Zhu, Y., & Wang, M. X. (2024). Kelp derived hierarchically porous carbon aerogels with ultrahigh surface area for high-energy-density supercapacitor in aqueous electrolyte. *Journal of Energy Storage*, 77, 109878. <https://doi.org/10.1016/j.est.2023.109878>
- Nayak, M. K., Sahoo, B. B., Thatoi, D. N., Nazari, S., Ali, R., & Chamkha, A. J. (2024). Recent advances on supercapacitor electrode materials from biowastes- a review. *Journal of Science: Advanced Materials and Devices*, 9(3), 100734. <https://doi.org/10.1016/j.jsamd.2024.100734>
- Nguyen, T. B., Yoon, B., Nguyen, T. D., Oh, E., Ma, Y., Wang, M., & Suhr, J. (2023). A facile salt-templating synthesis route of bamboo-derived hierarchical porous carbon for supercapacitor applications. *Carbon*, 206, 383–391. <https://doi.org/10.1016/j.carbon.2023.02.060>
- Okonkwo, C. A., Lv, T., Hong, W., Li, G., Huang, J., Deng, J., Jia, L., Wu, M., Liu, H., & Guo, M. (2020). The synthesis of micromesoporous carbon derived from nitrogen-rich spirulina extract impregnated castor shell based on biomass self-doping for highly efficient supercapacitor electrodes. *Journal of Alloys and Compounds*, 825, 154009. <https://doi.org/10.1016/j.jallcom.2020.154009>
- Raj, F. R. M. S., Boopathi, G., Jaya, N. V., Kalpana, D., & Pandurangan, A. (2020). N, S codoped activated mesoporous carbon derived from the Datura metel seed pod as active electrodes for supercapacitors. *Diamond and Related Materials*, 102, 107687. <https://doi.org/10.1016/j.diamond.2019.107687>
- Ramesh, A., Jeyavelan, M., Rajju Balan, J. A. A., Srivastava, O. N., & Leo Hudson, M. S. (2021). Supercapacitor and room temperature H₂, CO₂ and CH₄ gas storage characteristics of commercial nanoporous activated carbon. *Journal of Physics and Chemistry of Solids*, 152, 109969. <https://doi.org/10.1016/j.jpcs.2021.109969>
- Rawat, S., Jinlin, L., Ambalkar, A. A., Hotha, S., Muto, A., & Bhaskar, T. (2023). Syzygium cumini seed biochar for fabrication of supercapacitor: Role of inorganic content/ash. *Journal of Energy Storage*, 60, 106598. <https://doi.org/10.1016/j.est.2022.106598>

- Shanmuga Priya, M., Divya, P., & Rajalakshmi, R. (2020). A review status on characterization and electrochemical behaviour of biomass derived carbon materials for energy storage supercapacitors. *Sustainable Chemistry and Pharmacy*, 16, 100243. <https://doi.org/10.1016/j.scp.2020.100243>
- Wang, B., Jiao, R., Shi, F., Li, G., Zhou, J., Huang, Y., & Sun, W. (2023). Novel strategy for efficient conversion of biomass into N-doped graphitized carbon nanosheets as high-performance electrode material for supercapacitor. *Journal of Physics and Chemistry of Solids*, 181 111509. <https://doi.org/10.1016/j.jpccs.2023.111509>
- Wang, J., Zhang, X., Li, Z., Ma, Y., & Ma, L. (2020). Recent progress of biomass-derived carbon materials for supercapacitors. *Journal of Power Sources*, 451, 227794. <https://doi.org/10.1016/j.jpowsour.2020.227794>
- Wang, S., Zou, Y., Xu, F., Xiang, C., Peng, H., Zhang, J., & Sun, L. (2021). Morphological control and electrochemical performance of NiCo₂O₄@NiCo layered double hydroxide as an electrode for supercapacitors. *Journal of Energy Storage*, 41, 102862. <https://doi.org/10.1016/j.est.2021.102862>
- Wei, X., Wang, X., Wang, Y., Li, C., Bai, Q., Shen, Y., & Uyama, H. (2024). Biomass carbon aerogels by polyatomic synergistic modification and synchronous activation for supercapacitors. *Journal of Energy Storage*, 77, 110013. <https://doi.org/10.1016/j.est.2023.110013>
- Yang, X., Wang, Q., Lai, J., Cai, Z., Lv, J., Chen, X., Chen, Y., Zheng, X., Huang, B., & Lin, G. (2020). Nitrogen-doped activated carbons via melamine-assisted NaOH/KOH/urea aqueous system for high performance supercapacitors. *Materials Chemistry and Physics*, 250. <https://doi.org/10.1016/j.matchemphys.2020.123201>
- Yu, Q. X., Li, H. X., Wen, Y. L., Xu, C. X., Qin, S. F., Kuang, Y. F., Zhou, H. H., & Huang, Z. Y. (2023). The in situ formation of ZnS nanodots embedded in honeycomb-like N-S co-doped carbon nanosheets derived from waste biomass for use in lithium-ion batteries. *Xinxing Tan Cailiao/New Carbon Materials*, 38(3), 543–554. [https://doi.org/10.1016/S1872-5805\(23\)60726-7](https://doi.org/10.1016/S1872-5805(23)60726-7)
- Yu, Z., Wang, S., Huang, Y., Zou, Y., Xu, F., Xiang, C., Zhang, J., Xie, J., & Sun, L. (2022). Bi₂O₃ nanosheet-coated NiCo₂O₄ nanoneedle arrays for high-performance supercapacitor electrodes. *Journal of Energy Storage*, 55, 105486. <https://doi.org/10.1016/j.est.2022.105486>
- Yuan, Y., Cai, F., & Yang, L. (2022). Pore structure characteristics and fractal structure evaluation of medium- and high-rank coal. *Energy Exploration and Exploitation*, 40(1), 328–342. <https://doi.org/10.1177/01445987211034315>
- Zhou, H., Shu, R., Guo, F., Bai, J., Zhan, Y., Chen, Y., & Qian, L. (2021). N-O-P co-doped porous carbon aerogel derived from low-cost biomass as electrode material for high-performance supercapacitors. *Diamond and Related Materials*, 120, 108614. <https://doi.org/10.1016/j.diamond.2021.108614>
- Zhou, X., Liu, B., Chen, Y., Guo, L., & Wei, G. (2020). Carbon nanofiber-based three-dimensional nanomaterials for energy and environmental applications. *Materials Advances*, 1(7), 2163–2181. <https://doi.org/10.1039/d0ma00492h>